

Development of Empirical Relationships Between Input and Output Parameters of Sponge Iron Process Using Neural Network

A.K. Poonia¹, A.B. Soni¹, S. Khanam^{2*}

¹Department of Chemical Engineering, National Institute of Technology Raipur, Raipur, Chhattisgarh, India

²Department of Chemical Engineering, Indian Institute of Technology Roorkee, Roorkee, Uttarakhand, India

Abstract

In the present study, estimation of optimum input parameters corresponding to desired output parameters is carried out for a typical sponge iron process. For this purpose data of rotary kiln of the process are collected. It includes temperatures profiles inside the rotary kiln and flow rates of air, iron ore, feed coal, slinger coal and sponge iron. These data are analysed using ANN and group method of data handling (GMDH) approaches. Sixteen ANN topologies are proposed where TOP-3 is found best, which has mean absolute error (MAE) as 8.42. However, GMDH analysed the data with MAE of 8.72. Optimum values of operating parameters are found through ANN and GMDH approach and compared with that are used in the existing process. It shows that values of input parameters found through ANN can be selected as optimum based on minimum operating cost.

Keywords: ANN topologies, optimum input parameters, rotary kiln, sponge iron process

*Corresponding Author

E-mail: shabinahai@gmail.com

INTRODUCTION

The reduced iron exhibits a honeycomb structure, due to which it is named as sponge iron. It is seen that the growth of sponge iron industry in last few years is remarkable and today India is the largest producer of sponge iron as it covers 16% of global output.^[1,2] Sponge iron is produced primarily both using non-coking coal and natural gas as reductant and therefore classified based on coal and gas, respectively. With the promising availability of coal in India, sponge iron plants based on coal share major proportion of its production.

With the availability of raw materials, high demand of sponge iron and less payback period, sponge iron industry has emerged as a profitable venture. However, due to lack of proper integration techniques, non-

optimal process parameters and high energy consumption, the industries are facing a setback in the market. Amongst these drawbacks problems of proper integration and high energy consumption are addressed by many investigators.^[3-12] However, the optimization of input parameters based on desired output of the industry remains untouched. These parameters include temperature profile inside the rotary kiln and flow rate of sponge iron. These parameters depend on flow rate of air, iron ore and coal, which may be regulated to suit the desired output of the process. For this purpose one may use manual practice to observe the value of output parameter with the variation of input parameter. On the other hand, an easy methodology to optimize the input parameters is considered in the present work, which is neural network.^[13,14]

In the present work, industrial data of sponge iron process are analysed through 2 different neural network approaches *i.e.*, using artificial neural network (ANN) and group method of data handling (GMDH) algorithm. Using these optimum input parameters are found based on operating cost.

SPONGE IRON PROCESS

The schematic of sponge iron process is shown in Figure 1. Iron ore, coal and dolomite are fed to the kiln at controlled rates without pre-mixing and charge moves through the kiln (RK) depending upon rotation and inclination of the kiln. Air is also injected along the kiln length.^[9] There are two reduction reactions and five combustion reactions.

The material discharged from the kiln is cooled in rotary cooler (RC) using water sprayed over its shell. The cooler discharge is then separated into sponge

iron, char and ash through magnetic separator. Waste gas generated in the rotary kiln is passed through dust settling chamber (DSC). Further, CO produced through incomplete oxidation in RK is converted to CO₂ using excess air in after burning chamber (ABC) as shown in Figure 1. Waste gas, which exits the ABC, is passed through waste heat recovery boiler (WHRB) to produce steam for power generation. Further, it is passed through electro static precipitator (ESP) for dust removal and then released to the atmosphere through chimney. The flow of waste gas from rotary kiln to chimney is maintained using an induced draft fan located beneath the chimney.

As the aim of the present work is to correlate the input and output parameters of the sponge iron process using neural networks, data of primary unit of process *i.e.*, rotary kiln is collected.

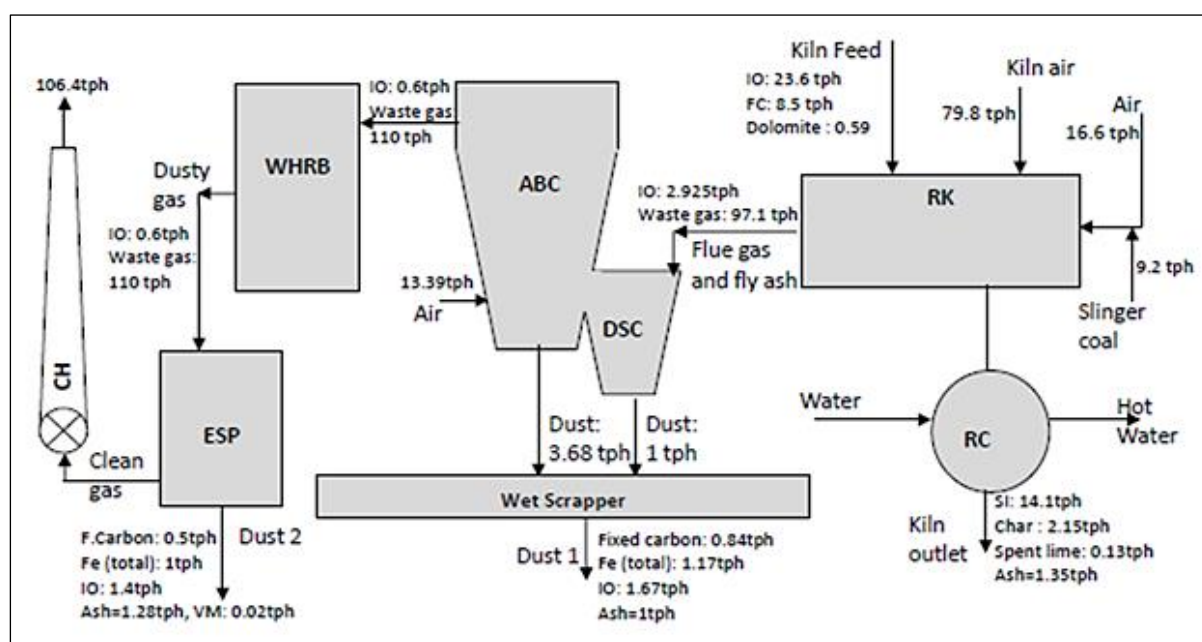


Fig. 1. Process Flow Diagram of Sponge Iron Process.

DATA COLLECTION

The schematic of rotary kiln is shown in Figure 2. The temperatures, T1 to T12, of the kiln are observed through 12 thermocouples placed along the length of the kiln. These values show temperature

profile inside the kiln. Around the periphery of the kiln air is injected through positions, AT1, AT2, AT3, MF1 and MF2, as shown in Figure 2. At AT1 to AT3 one blower is attached to each position whereas, at MF1 and MF2 two blowers are

placed to each inlet. Thus, total seven blowers are placed. To produce sponge iron, iron ore and coal are used as raw materials. In the kiln coal is injected from feed as well as discharge ends, which is called feed coal and slinger coal, respectively, as shown in Figure 1. Slinger coal is fed pneumatically in different sizes such as fine, medium and coarse, whereas, feed coal is fed as coarse. This is due to the process requirement.

For the present work data of a typical Indian sponge iron industry with production capacity of 350 tpd is collected on per hour basis. There are 440 data points, which are collected for 24 hours for 18 days and 8 hours of 19th day. It shows that flow rate of air is represented in terms

of % damper opening of blower such as 20, 19, 43, etc. Damper opening of 1% shows air flow rate around $600\text{m}^3/\text{h}$. Before using these data for analysis, mass balance is performed for all 440 data points, which shows maximum deviation of 5.4%. It is not significant and thus, all 440 data points are considered for further analysis.

The data consists of ten input parameters such as IO, FC, FSC, MSC and CSC and flow rate of air at position AT1, AT2, AT3, MF1 and MF2. It also contains 13 output parameters as T1, T2, T3, T4, T5, T6, T7, T8, T9, T10, T11, T12 and SI. The operating ranges of input and output parameters, found for 440 data points, are summarized in Table 1.

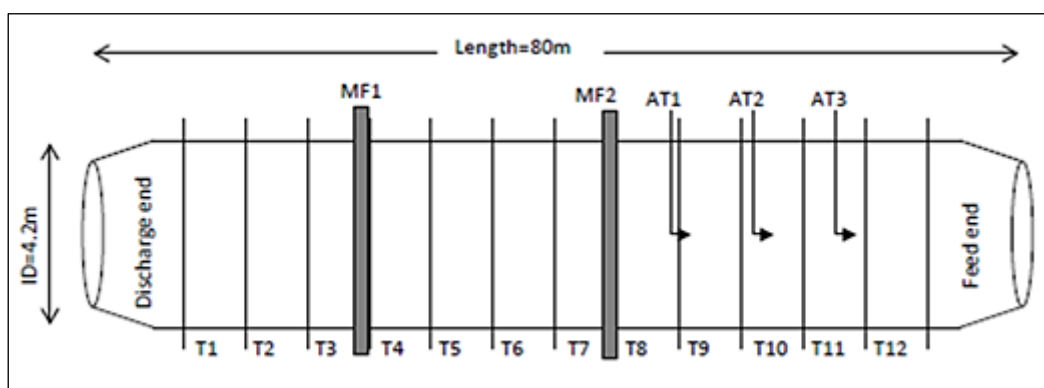


Fig. 2. Schematic of Rotary Kiln.

Table 1. Operating Ranges of Input and Output Parameters.

Parameter	Operating range	Parameter	Operating range
IO	21–23.8 tph	T1	1002–1108°C
FC	8.2–8.8 tph	T2	986–1098°C
FSC	1.7–1.9 tph	T3	976–1091°C
MSC	2.65–4 tph	T4	992–1092°C
CSC	2.9–3.9 tph	T5	1015–1109°C
SI	13.53–15.355 tph	T6	1019–1102°C
AT1	16–20%	T7	1002–1097°C
AT2	19–21%	T8	1000–1098°C
AT3	3–14%	T9	862–991°C
MF1	43–53%	T10	829–955°C
MF2	20–23%	T11	764–911°C
		T12	700–800°C

DATA ANALYSIS APPROACH

In the present work input and output parameters of rotary kiln are correlated through different approaches such as artificial neural network (ANN) and group method of data handling (GMDH) method.

The ANN Approach

Development of ANN Topologies

As ANN approach provides relationship between input and output parameters it affects by varying a few factors such as randomization, number of hidden layers, type of models, type of functions, number of epochs, etc. Considering these factors sixteen ANN topologies are developed as reported in Table 2. As more number of hidden layers complexes the solution, only up to two is considered in these topologies. Multilayer perceptrons (MLP) and Radial basis function (RBF) models are used as these are most suited to handle random industrial data. Moreover, TanhAxon and SigmoidAxon are accounted as different functions through which input and output parameters are correlated.

These topologies are solved using NeuroSolutions 4.0 software. For this purpose 2/3rd of data points are used as training and rest as testing. So, amongst 440 data points 295 and 145 are considered for training and testing, respectively. The performance of a topology is defined by two parameters such as Normalized Mean Square Error (NMSE) and the correlation coefficient (R) defined through Eqs. 1 and 2.^[15] The values of NMSE and R should be minimum and close to unity, respectively, for optimum topology.

$$NMSE = \frac{PN(MSE)}{\sum_{j=0}^P \left[N \sum_{i=0}^N d_{ij}^2 - \left(\sum_{i=0}^N d_{ij} \right)^2 \right]} \quad (1)$$

$$R = \frac{\sum_{i=0}^N (y_i - \bar{y})(d_i - \bar{d})}{\sqrt{\frac{\sum_{i=0}^N (y_i - \bar{y})^2}{N} \frac{\sum_{i=0}^N (d_i - \bar{d})^2}{N}}} \quad (2)$$

Though ANN correlates the input and output parameters and provides value of R for each output parameters, it is very difficult to prepare governing equations of output parameters as a function of input parameters. This problem is further enhanced if significant number of parameters interacts with each other. Thus, to find the governing equations of output parameters GMDH approach is used, which is based on neural network.

The GMDH Algorithm

The correlation between various input and output parameters are developed using GMDH algorithm based on Volterra functional series^[16] as:

$$y = a_0 + \sum a_i x_i + \sum \sum a_{ij} x_i x_j + \sum \sum \sum a_{ijk} x_i x_j x_k + \dots \quad (3)$$

Where, i,j,k vary from 1 to m

During modelling GMDH algorithm involves four heuristics rules as:

- To collect a set of data points that seems to be relevant to the object.
- It divides data points into 2 groups. First is used to estimate the coefficients of model whereas, the second separates information embedded in the data into either useful or harmful.
- It creates a set of elementary functions where complexity will increase through an iterative procedure producing different models.
- It applies an external criterion to choose the optimum model using Gödel's incompleteness theorem.^[17]

Ivakhnenko^[18] claimed that the self-organization is necessary if it is impossible to trace all input-output relationships

through an entire system which is too complex. This ability made GMDH algorithm an appropriate modelling procedure for real world systems.^[16]

RESULTS AND DISCUSSION

As the present work analyses data of rotary kiln through ANN topologies and GMDH approach, the results found using these are discussed in subsequent paragraphs:

ANN Topologies

Topologies, TOP-1 to TOP-16, are proposed for complete data as shown in Table 2. For these topologies the average values of R, computed using R values of individual output parameters, T1 to T12

and SI, are plotted in Figure 3. It shows that average value of R is maximum for topology, TOP-3, which is found as 0.8026 using 1000 epochs. When TOP-3 is trained with increased number of epochs as 2000, 3000, 4000 and 5000 the average value of R is found as 0.8147, 0.7902, 0.7823 and 0.7999, respectively. Thus, it is maximum for 2000 epochs. For this topology, average values of mean absolute error (MAE) and NMSE are found as 8.42 and 0.333, respectively. The average MAE and NMSE is based on MAE and NMSE of individual output parameter such as T1, T2, T3, T4, T5, T6, T7, T8, T9, T10, T11, T12 and SI as shown in Table 3.

Table 2. Topologies for ANN Network.

S. no.	Networks tested for present work	Randomization	No. of hidden layers	Model	Function
1	TOP-1	1	1	MLP	TanhAxon
2	TOP-2	1	1	MLP	SigmoidAxon
3	TOP-3	1	1	RBF	TanhAxon
4	TOP-4	1	1	RBF	SigmoidAxon
5	TOP-5	2	1	MLP	TanhAxon
6	TOP-6	2	1	MLP	SigmoidAxon
7	TOP-7	2	1	RBF	TanhAxon
8	TOP-8	2	1	RBF	SigmoidAxon
9	TOP-9	1	2	MLP	TanhAxon
10	TOP-10	1	2	MLP	SigmoidAxon
11	TOP-11	1	2	RBF	TanhAxon
12	TOP-12	1	2	RBF	SigmoidAxon
13	TOP-13	2	2	MLP	TanhAxon
14	TOP-14	2	2	MLP	SigmoidAxon
15	TOP-15	2	2	RBF	TanhAxon
16	TOP-16	2	2	RBF	SigmoidAxon

Table 3. Testing Report for Data-1.

Parameter	SI	T1	T2	T3	T4	T5	T6	T7	T8	T9	T10	T11	T12
NMSE	0.18	0.13	0.14	0.13	0.52	0.33	0.64	0.37	0.38	0.48	0.34	0.38	0.30
MAE	0.09	8.42	8.71	8.77	9.73	7.19	7.15	10.33	9.50	10.55	9.86	9.94	9.26
R	0.91	0.93	0.93	0.93	0.71	0.82	0.60	0.80	0.79	0.72	0.81	0.79	0.84

It is observed that for the present data the maximum value of R is found as 0.8147 through ANN, which is not very significant. It is due to large variation in

input and output parameters. For example, temperature, T1, varies from 1108 to 1002°C, which is 9.57%, as shown in Table 1. Similarly, other output parameters

such as T2, T3, T4, T5, T6, T7, T8, T9, T10, T11, T12 and SI vary by 10.2%, 10.5%, 9.16%, 8.48%, 7.53%, 10.1%, 13%, 13.2%, 16.1%, 12.5% and 12%, respectively.

In the similar pattern variations in input parameters such as flow rate of air at positions, AT1, AT2, AT3, MF1 and MF2, and IO, FC, FSC, MSC and CSC are observed as 20%, 9.524%, 78.6%, 18.87%, 13.04%, 11.8%, 6.8%, 10.5%, 33.8% and 25.6%, respectively. It is to be noted that variation in flow rate of air at AT3 is maximum, i.e. 78.6%, as maximum and minimum values of % of damper opening for AT3, reported in Table 1, are 14 and 3, respectively. These are corresponding to 8400 m³/h to 1800 m³/h.

As topology, TOP-3, with 2000 epochs shows best average value of R it is used for further analysis. The operating range of output parameters, T1 to T12 and SI, predicted for TOP-3 is shown in Table 4. These ranges are found based on minimum and maximum values of output parameters predicted while testing.

In fact, the value of maximum temperature in output parameters, T1 to T12, predicted through software is 1094.9°; whereas, it was 1109° in industrial data shown in Table 1. This meets the process requirement as accretion formation inside the kiln starts at 1100°C. It is due to low melting point compounds available in the kiln such as FeO, SiO₂, Al₂O₃ and CaO or MgO.

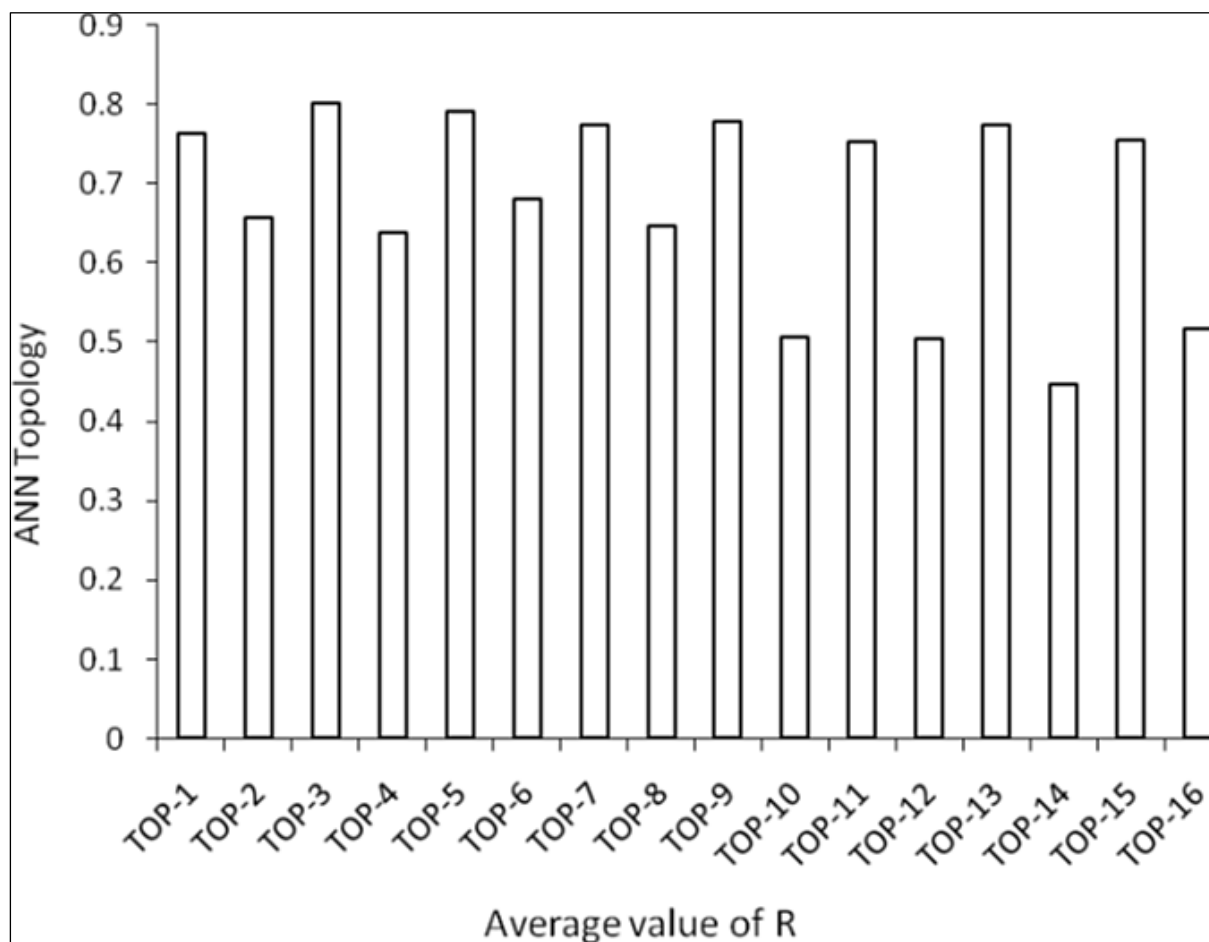


Fig. 3. Values of R for Different ANN Topologies Proposed for Complete Data.

Table 4. Ranges of Output Parameters Predicted for Complete Data.

Output parameter	Operating range
SI	13.7–15.4 t/h
T1	1004.7–1092°C
T2	989.3–1081.7°C
T3	978.2–1075.5°C
T4	1020.7–1078.9°C
T5	1048–1094.9°C
T6	1052.9–1090.4°C
T7	999.3–1070.3°C
T8	972.4–1035°C
T9	912.9–966°C
T10	865.2–928.5°C
T11	800.5–857.8°C
T12	728.7–788.4°C

Selection of Best Value of Input Parameters Using ANN

The operating ranges of output parameters, predicted for best ANN topology, TOP-3, are shown in Table 4. These ranges of output parameters should be maintained during the process, which can be achieved in the process by adjusting input parameters.

However, it is not known a priori that how each input parameter must be set to find desired value of output parameter. For this purpose one should observe output parameters while varying values of input parameters. It is a cumbersome approach which requires considerable experimentation to set the optimum input parameters.

Thus, a better option is to predict values of input parameters correspond to desired output using ANN topologies. For this purpose parameters, T1, T2, T3, T4, T5, T6, T7, T8, T9, T10, T11, T12 and SI, are considered as input whereas IO, FC, FSC, MSC, CSC, AT1, AT2, AT3, MF1 and MF2 are accounted as output parameters.

Further, the values of T1, T2, T3, T4, T5, T6, T7, T8, T9, T10, T11, T12 and SI for all data points are varied in such a manner so that all values of these parameters should fall within the operating range shown in Table 4.

For example, if value of T1 in industrial data is 990°C, it is replaced with 1004.7°C shown in Table 4. For these parameters, values of output parameters are found using Neurosolutions 4.0, which should be the input parameters for desired range of output parameters shown in Table 4.

For this purpose, topologies, TOP-1 to TOP-16, are solved and the average values of R are shown in Figure 4. It shows that value of R is maximum for topology, TOP- 5, which is predicted as 0.8621 for 1000 epochs. When topology, TOP-5, is trained with 2000, 3000, 4000 and 5000 number of epochs the average value of R is found as 0.8791, 0.7674, 0.8513 and 0.8161, respectively.

Thus, TOP-5 with 2000 epochs is found as best. Based on this analysis the average values of output parameters, IO, FC, FSC, MSC, CSC, AT1, AT2, AT3, MF1 and MF2, are found as 23.4 tph, 8.7 tph, 1.8 tph, 3.6 tph, 3.5 tph, 11,391.9 m³/h, 11,857.2 m³/h, 3602.2 m³/h, 31,110.9 m³/h and 12,772.7 m³/h, respectively.

As these values correlate the output with appreciable value of R, i.e. 0.8791, these are considered as most suitable values of input parameters for desired range of output parameters shown in Table 4.

Thus, these values of input parameters are considered to be optimum for the present industrial data found.

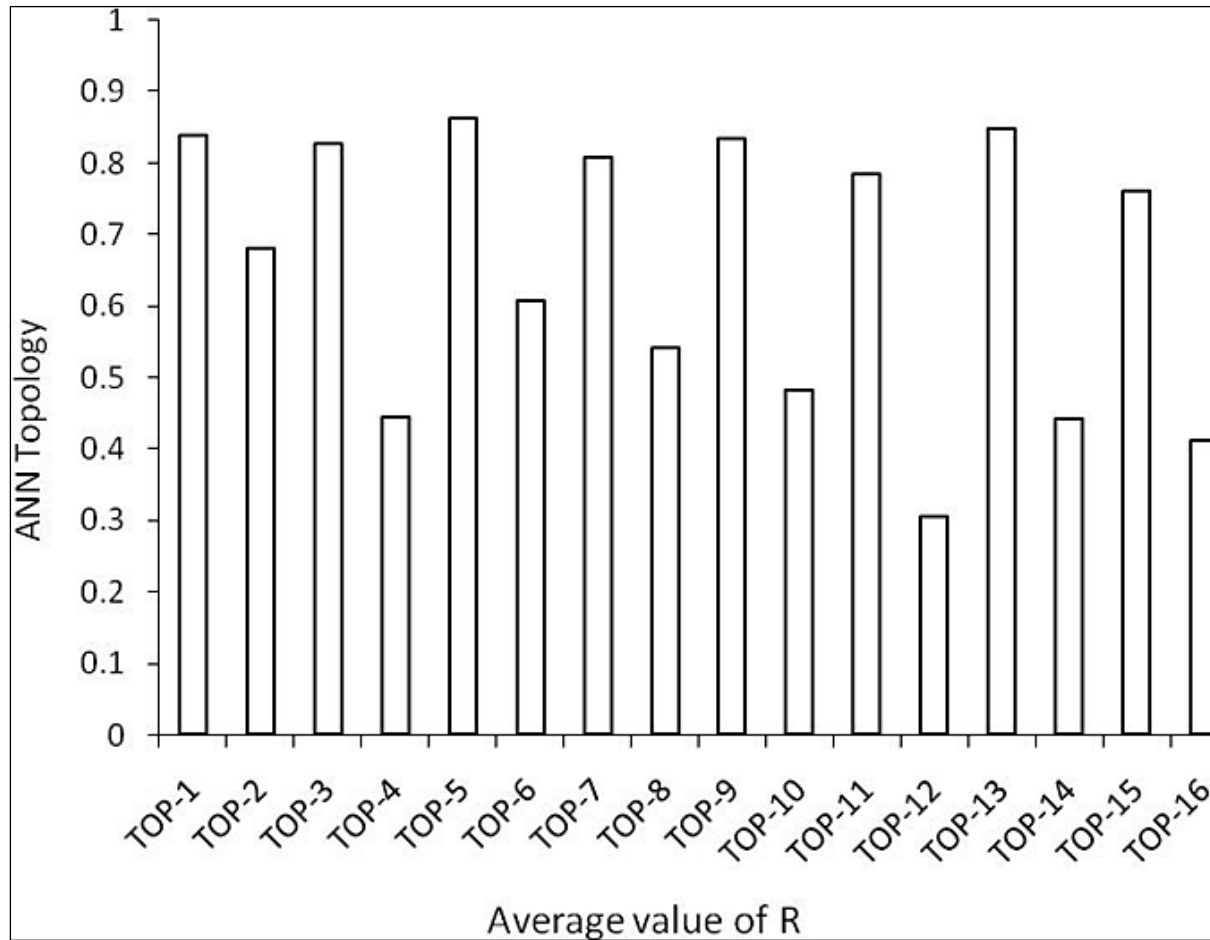


Fig. 4. Average Values of R for ANN Topologies Developed When T1 to T12 and SI Are Treated as Input Parameters.

Analysis of Data Using GMDH Algorithm

In this approach input and output parameters of rotary kiln are analysed using software, GMDH Shell version 2.6.6, with regression neural type algorithm. In this analysis data of rotary kiln with ten input and thirteen output parameters is considered. Two hidden layers and neuron function of two degree with neuron complexity up to 2 are used for simulation. The result shows the value of average MAE as 8.72. The equations of output parameters as functions of input parameters based on Eq. 3 are:

For output parameter, T1

$$T1 = 3198 + 4.8 \times x - 0.001962 \times x^2 - 9.905 \times y + 0.004873 \times y^2 \quad (4)$$

$$y = -9364 + 439.4 \times IO - 0.01796 \times IO \times MF1 + 0.425 \times MF1 \quad (5)$$

$$x = -746.6 + 995 \times CSC - 0.02808 \times CSC \times AT3 - 141.3 \times (CSC)^2 + 0.1281 \times AT3 - 3.66 \times 10^{-6} \times (AT3)^2 \quad (6)$$

For output parameter, T2

$$T2 = 3095 + 13.08 \times x - 0.03698 \times x \times y + 0.01244 \times y^2 - 18.07 \times y + 0.0274 \times y^2 \quad (7)$$

$$x = -1028 + 890.1 \times CSC - 0.04294 \times CSC \times AT1 - 73.02 \times CSC^2 + 0.1375 \times AT1 \quad (8)$$

$$y = -1.413 \times 10^4 + 1196 \times IO - 27.93 \times (IO)^2 + 0.1574 \times MF1 - 2.504 \times 10^{-6} \times (MF1)^2 \quad (9)$$

For output parameter, T3

$$T3 = 1341 + 11.25 \times x - 0.05682 \times x \times y + 0.02318 \times y^2 - 12.89 \times y + 0.0349 \times y^2 \quad (10)$$

$$x = 1709 - 908.5 \times FSC + 121.8 \times FSC \times CSC + 121.5 \times (FSC)^2 + 220.2 \times CSC$$

$$-78.97 \times (CSC)^2 \quad (11)$$

$$y = -8867 + 420.6 \times IO - 0.01719 \times IO \times MF1 + 0.4043 \times MF1 \quad (12)$$

For output parameter, T4

$$T4 = 2.811 \times 10^4 + 44.72 \times x - 0.0418 \times x \times y - 97.22 \times y + 0.06725 \times y^2 \quad (13)$$

$$x = 2.892 \times 10^4 - 6275 \times FC + 169.1 \times FC \times CSC + 339.7 \times (FC)^2 - 838 \times CSC - 97.03 \times (CSC)^2 \quad (14)$$

$$y = 3501 - 0.4532 \times AT1 + 1.489 \times 10^{-6} \times AT1 \times AT3 + 2.065 \times 10^{-5} \times (AT1)^2 - 1.424 \times 10^{-6} \times (AT3)^2 \quad (15)$$

For output parameter, T5

$$T5 = 2.069 \times 10^4 + 20.29 \times x - 0.018 \times x \times y - 57.87 \times y + 0.03598 \times y^2 \quad (16)$$

$$x = 1465 - 0.04625 \times AT3 + 4.402 \times 10^{-6} \times AT3 \times MF2 - 8.32 \times 10^{-7} \times (AT3)^2 - 0.0317 \times (MF2) \quad (17)$$

$$y = 1846 - 1011 \times FSC - 0.08869 \times FSC \times AT2 + 595.5 \times FSC^2 + 7.22 \times 10^{-6} \times (AT2)^2 \quad (18)$$

For output parameter, T6

$$T6 = -6.44 \times 10^4 + 0.0004133 \times x^2 + 121.2 \times y - 0.0565 \times y^2 \quad (19)$$

$$x = -6560 + 0.3439 \times AT3 - 9.97 \times 10^{-6} \times AT3 \times MF1 - 4.601 \times 10^{-6} \times (AT3)^2 + 0.455 \times MF1 - 6.797 \times 10^{-6} \times (MF1)^2 \quad (20)$$

$$y = -0.1077 \times AT2 - 8.479 \times 10^{-7} \times AT2 \times MF2 + 5.1 \times 10^{-6} \times (AT2)^2 + 0.2709 \times MF2 - 1.04 \times 10^{-5} \times (MF2)^2 \quad (21)$$

For output parameter, T7

$$T7 = -1491 + 0.3402 \times AT3 - 0.00035 \times AT3 \times x + 2.882 \times 10^{-6} \times (AT3)^2 + 2.483 \times x \quad (22)$$

$$x = -6949 - 239.4 \times IO \times CSC + 15.51 \times (IO)^2 + 5234 \times CSC + 64.74 \times (CSC)^2 \quad (23)$$

For output parameter, T8

$$T8 = -3.24 \times 10^4 + 64.71 \times x - 0.02145 \times x \times y - 0.0212 \times x^2 + 0.7536 \times y + 0.0106 \times y^2 \quad (24)$$

$$x = 3336 - 1149 \times MSC + 0.0326 \times MSC \times AT3 + 145.9 \times (MSC)^2 - 0.1667 \times AT3 + 5.57 \times 10^{-6} \times (AT3)^2 \quad (25)$$

$$y = -2865 + 369.3 \times CSC - 0.06198 \times CSC \times AT2 + 62.72 \times (CSC)^2 + 0.5193 \times AT2 - 1.269 \times 10^{-5} \times (AT2)^2 \quad (26)$$

For output parameter, T9

$$T9 = -8.17 \times 10^4 + 0.1935 \times AT3 - 0.0002114 \times AT3 \times x + 1.462 \times 10^{-6} \times (AT3)^2 + 172.6 \times x - 0.09007 \times x^2 \quad (27)$$

$$x = 2284 - 438.2 \times CSC + 0.0366 \times CSC \times MF2 - 0.1135 \times MF2 \quad (28)$$

For output parameter, T10

$$T10 = -6845 + 16.24 \times x - 0.008809 \times x^2 + 0.0003269 \times y^2 \quad (29)$$

$$x = 5046 + 0.1292 \times MF1 \times CSC - 7.207 \times 10^{-6} \times (MF1)^2 - 2479 \times CSC - 209.5 \times (CSC)^2 \quad (30)$$

$$y = 0.3154 \times AT3 - 0.01388 \times AT3 \times IO + 1.525 \times 10^{-6} \times (AT3)^2 - 50.08 \times IO + 3.778 \times (IO)^2 \quad (31)$$

For output parameter, T11

$$T11 = -2.208 \times 10^4 + 20.28 \times x - 0.02341 \times x \times y + 33.22 \times y - 0.00779 \times y^2 \quad (32)$$

$$x = 5327 - 2660 \times CSC + 0.1387 \times CSC \times MF1 - 228.9 \times CSC^2 - 7.73 \times 10^{-6} \times (MF1)^2 \quad (33)$$

$$y = 2604 - 880.9 \times MSC + 0.023 \times MSC \times AT3 + 114.1 \times MSC^2 - 0.1258 \times AT3 \times 5.002 \times 10^{-6} \times (AT3)^2 \quad (34)$$

For output parameter, T12

$$T12 = -1.307 \times 10^4 + 0.03408 \times AT2 - 0.0002954 \times AT2 \times x + 8.331 \times 10^{-6} \times (AT2)^2 + 34.46 \times x - 0.0195 \times x^2 \quad (35)$$

$$x = -263.7 + 453.4 \times CSC - 0.0286 \times CSC \times AT3 - 43.56 \times (CSC)^2 + 0.0832 \times AT3 \times 1.66 \times 10^{-6} \times (AT3)^2 \quad (36)$$

For output parameter, SI

$$SI = -47.93 + 0.0064 \times AT3 - 0.00039 \times AT3 \times x - 3.51 \times 10^{-8} \times (AT3)^2 + 4.113 \times x \quad (37)$$

$$x = 496 - 81.22 \times FC + 11.66 \times FC \times CSC + 2.867 \times (FC)^2 - 97.19 \times CSC - 0.513 \times (CSC)^2 \quad (38)$$

Table 5. Operating Ranges and % Error Involved in Equations.

Output parameter	Eq. no.	Operating range	% error	Input parameters
T1, °C	11, 12, 13	1002–1108	–6.4	CSC, AT3, IO, MF1
T2, °C	14, 15, 16	986–1098	–5.5	CSC, AT1, IO, MF1
T3, °C	17, 18, 19	976–1091	–10.3	FSC, CSC, IO, MF1
T4, °C	20, 21, 22	992–1092	4.42	FC, CSC, AT1, AT3
T5, °C	23, 24, 25	1015–1109	4.13	AT3, MF2, FSC, AT2
T6, °C	26, 27, 28	1019–1102	–4.14	AT3, MF1, MF2, AT2
T7, °C	29, 30	979–1089	1.9	IO, CSC, AT3
T8, °C	31, 32, 33	942–1052	7.13	MSC, AT3, CSC, AT2
T9, °C	34, 35	862–991	8.54	CSC, MF2, AT3
T10, °C	36, 37, 38	829–955	–9.6	MF1, CSC, AT3, IO
T11, °C	39, 40, 41	764–911	–9.5	CSC, MF1, MSC, AT3
T12, °C	42, 43	700–800	10.2	CSC, AT2, AT3
Flow rate of SI, t/h	44, 45	13.53–15.355	–4.8	FC, CSC, AT3

The operating ranges of these equations as well as maximum % error is summarized in Table 5. The % error is computed for each data point and maximum deviation between values obtained from industry and that predicted using respective equations is reported in Table 5. It shows that the maximum % error within operating range of equations is found as $\pm 10.5\%$.

Selection of Best Value of Input Parameters Using GMDH

Equations 4 to 38 are used to find the feasible region of input parameters. The parameters used to plot the feasible region should be those which affect maximum number of output parameters. It is evident from Table 5 that amongst 13 output parameters, input parameters such as IO,

FC, FSC, MSC, CSC, AT1, AT2, AT3, MF1 and MF2 affect 5, 2, 2, 2, 11, 2, 3, 11, 6 and 3 number of output parameters. It shows that CSC and AT3 affect maximum number of output parameters, which are 11. Thus, feasible region is plotted between CSC vs. AT3.

In this region optimum values of input parameters are found based on minimum operating cost. Amongst ten input parameters only five such as IO, FC, FSC, MSC and CSC are accounted in the operating cost. Hence, these parameters are plotted in the feasible region as shown in Figure 5. It indicates the CSC and air flow rate at position, AT3, for different FC, IO and MSC. The values of CSC and AT3 for different FC are found using

equations Eqs. 13, 14 and 15. Similarly, curves for different values of IO and MSC are plotted using equations developed for parameters, T7 and T8, respectively.

The ranges of FC, IO and MSC, considered in Figure 5, are based on values obtained from industrial data. To compute values of CSC and AT3 constant values of

T4, T7 and T8, found through averaging the values of operating range shown in Table 5, are used. In fact, amongst five input parameters, IO, FC, FSC, MSC and CSC, FSC is not shown in Figure 5 as it is small in amount. Therefore, the average value of FSC as 1.8 tph, found using its operating range shown in Table 1, is used while computing the operating cost.

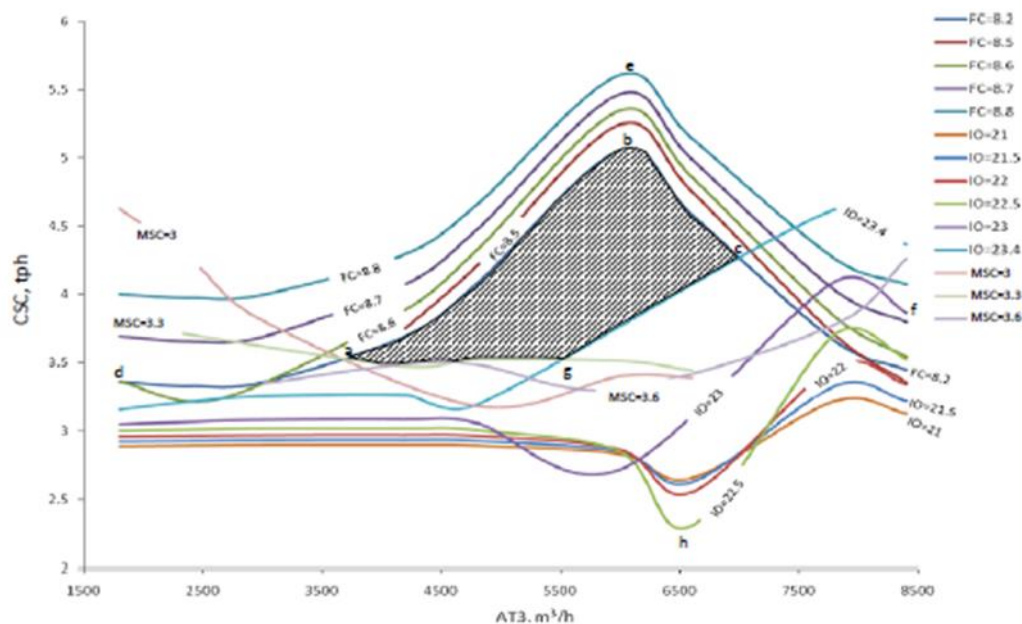


Fig. 5. Feasible Region for Different Input Parameters.

Figure 5 shows that at constant value of FC as flow rate of AT3 increases the value of CSC first increases and then decreases. The plausible explanation is that as AT3 increases more amount of oxygen enters the kiln, which enhances the requirement of coal to carry out combustion in the kiln. As value of FC is fixed increased demand of coal is supplied through CSC. Further, increase in flow rate of AT3 may cause some of coal particle to leave the kiln with waste gas. Due to this at higher flow rate of AT3 value of CSC decreases. Figure 5 also shows that at fixed value of IO, amount of CSC is not affected by AT3 up to certain value.

Further, it decreases and then increases with increase in AT3. It is so at higher flow rate of air at AT3 some amount of

coal may leave the kiln along with waste gas. The reduced amount of coal is supplied additionally. Thus, for increased flow rate of air at AT3 a significant amount of coal is supplied, which causes sharp increase in CSC. Further, it is noted that more value of IO causes more reduction to occur, which requires more amount of coal. Due to this at increased value of IO, amount of CSC also increases. Similar explanation can be illustrated for MSC. Figure 5 indicates the feasible region through shaded area. It is surrounded by curves of input parameters such as FC, IO and MSC.

To compute the values of input parameters where operating cost is minimum a few data points are collected from Figure 5

within or outside the feasible region. These points are indicated through 'a' to 'h' as shown in Figure 5. For these points values of different input parameters along with operating costs are predicted and shown in Table 6. The operating cost is computed using cost of iron ore and coal as Rs 5080/ton and Rs 3900/ton, respectively. It is assumed that cost of all sizes of coal is equal.

Table 6 shows that operating cost is minimum for values of input parameters at point 'a'. In fact the operating cost shown in Table 6 should also include cost of FSC. As it is maintained at constant value of 1.8tph it increases the operating cost for each point without changing the order as far as minimum operating cost is concerned. Further, it is observed that values of input parameters at points 'g' and 'h' shown in Figure 5 are not included in Table 6. It is due to the fact that if FC is computed for a value below to 8.2 tph the amount of coal in kiln reduces significantly which will be supplied by

CSC.

Consequently, the amount of CSC will increase. Thus, for value of FC less than 8.2 tph curve will be drawn above to the plot of FC equal to 8.2 tph and hence, it cannot reach to points 'g' and 'h'. Therefore, curve of FC does not appear below to the line of 8.2 tph. Moreover, the operating range of FC is from 8.2 tph to 8.8 tph as shown in Table 1 and thus, FC is not considered below to 8.2 tph in Figure 5.

Based on operating cost optimum values of input parameters are found at point 'a' as shown in Table 6. Further, it is observed that values of FC, IO and MSC are plotted in Figure 5 using equations for T4, T7 and T8, respectively. The % errors for predicting these temperatures are 4.42%, 1.9% and 7.13% as shown in Table 5. Considering these the revised values of FC, IO and MSC are found as 8.6, 23.9 and 8.8 tph, respectively.

Table 6. Input Parameters and Operating Cost at Different Data Points Shown in Figure 5.

Data point	Input parameter (tph)				Operating cost (Rs/ton)
	FC	MSC	CSC	IO	
a	8.2	3.3	3.5	23.5	176,710
b	8.2	2.28	5.05	24.14	183,198.2
c	8.2	2.46	4.2	23.4	176,826
d	8.6	3.2	3.35	23.5	178,465
e	8.8	2.1	5.6	24.26	187,590.8
f	8.6	3.4	3.75	23.0	178,265

Comparison of Results of ANN and GMDH

The values of optimum input parameters found through ANN and GMDH are compared with that are used in the existing process as shown in Figure 1. The results of comparison are summarized in Table 7. It shows that % deviation between values

used in Figure 1 and found through ANN is less than 3.5%, whereas that predicted using GMDH is within $\pm 4.5\%$. Thus, optimum values of input parameters found through ANN can be used in the process. This fact is also supported through operating cost as it is minimum for the values predicted using ANN.

Table 7. Comparison of Optimum Values of Input Parameters With That Are Used in the Process.

Operating parameter	Shown in Fig. 1	Optimum input parameters predicted through ANN		% Deviation while comparing with	
		ANN	GMDH	ANN	GMDH
Iron ore	23.61 tph	23.4 tph	23.9 tph	0.89	-1.2
Feed coal	8.5 tph	8.7 tph	8.6 tph	-2.4	-1.2
Slinger coal	9.2 tph	8.9 tph	8.8 tph	3.3	4.3
Air through position, AT1, AT2, AT3, MF1 and MF2	79.8 tph	70,734.9 m ³ /h (i.e. 79.223 tph)	81.78 tph	0.72	-2.5
Operating cost, Rs/ton	188,969	187,512	189,272	0.77	-0.16

CONCLUSIONS

The salient features of the study are shown below:

- For data of rotary kiln topology, TOP-3, with 2000 epochs shows best average value of R as 0.8147. For this topology MAE and NMSE are 8.42 and 0.333, respectively.
- The data are analysed using GMDH algorithm with MAE value of 8.72. Governing equations are developed for thirteen output parameters with maximum % error as $\pm 10.5\%$.
- The tested output parameters meet the process requirements.
- Based on % deviation and operating cost values of input parameters found through ANN are selected as optimum.

Nomenclature

- a_i Vector of weights
 CSC Flow rate of coarse slinger coal, tph
 d_i Desired response for i th exemplar
 d_{ij} Desired output for exemplar 'i' at processing element 'j'
 \bar{d} Mean desired value for the dataset considered
 $x=(x_1, x_2, \dots, x_m)$ Input variables vector
 y_i Network output for exemplar 'i'

\bar{y} Mean network output value for the data set considered

REFERENCES

- www.spongeironindia.in/prodfig06-07.html.
- Comprehensive Industry Document Series COINDS, Comprehensive Industry Document on iron ore mining. Aug/2007-08.
- Rani Devi S., Mazumder B., Recovery of carbon from sponge iron plants – studies on the dust samples, *Environ Sci Eng.* 2007; 5: 11–6p.
- Misra H.P., Ipicol B. Indian sponge iron production – problems and solutions, *SGAT Bull.* 2006; 7: 37–46p.
- Steinmetz E., Thielmann R. Present state and development potential of processes for the direct reduction and smelting reduction of iron ores, *Metall Plant Technol.* 1986; 3: 24p.
- Agrawal B.B., Prasad K.K., Sarkar S.B., *et al.* Cold bonded ore-coal composite pellets for sponge ironmaking. Part 1 Laboratory scale development, *Ironmaking Steelmaking.* 2000; 27: 421–5p.
- Agrawal B.B., Prasad K.K., Sarkar S.B., *et al.* Cold bonded ore-coal

- composite pellets for sponge ironmaking. Part 2. Plant trials in rotary kiln, *Ironmaking Steelmaking*. 2001; 28: 23–6p.
8. Eriksson K., Larsson M. *Energy Survey of the Sponge Iron Process*. Sweden, 2005.
 9. Biswas D.K., Asthana S.R., Rau V.G. Some studies on energy savings in sponge iron plants, *Trans. ASME*. 2003; 125: 228–37p.
 10. Chatterjee A., Biswas D.K. Axial rotary and radial injection of air in preheating zone of a kiln, *Trans Indian Inst Met*. 1989; 42: 281–9p.
 11. Bandyopadhyay A., Ray A.K., Srivastava M.P., et al. Selection of coals for rotary kiln sponge iron plant, *Trans Indian Inst Met*. 1987; 40: 209–18p.
 12. Agarwal V.P., Sood K.C., Direct reduction through coal route and power generation from the kiln waste gases, *Trans Indian Inst Met*. 1996; 3: 51–6p.
 13. Dobrazanski L.A., Honysz R., Application of ANN in modeling of normalized structural steels mechanical properties, *J Achieve Mater Manuf Eng*. 2009; 32: 1p.
 14. Chen J.C., Chang N.B., Shieh W.K. Assessing wastewater reclamation potential by neural network model, *Eng Appl Art Intel*. 2003; 16: 149–57p.
 15. Van Ooyen A., Nienhuis B. Improving the convergence of the back-propagation algorithm, *Neural Net*. 1992; 5: 465–71p.
 16. Anastasakis L., Mort N. *The Development of Self-Organization Techniques in Modeling: A Review of the Group Method of Data Handling (GMDH)*. Research Report no. 813, Department of Automatic Control and systems engineering, University of Sheffield, October 2001.
 17. Kozen D.C., *Gödel's Incompleteness Theorem, Automata and Computability*. New York: Springer; 1997, 282–6p.
 18. Ivakhnenko A.G. The group method of data handling – a rival of the method of stochastic approximation, *Soviet Automatic Control c/c of Avtomatika*. 1968; 1, 3: 43–55p.